JCTC Journal of Chemical Theory and Computation

Peculiarities of the Electronic Structure of Cytochrome P450 Compound I: CASPT2 and DFT Modeling†

Mariusz Radoń

Department of Theoretical Chemistry, Jagiellonian University, Ingardena St. 3, 30-060 Cracow, Poland

Ewa Broclawik*

Institute of Catalysis and Surface Chemistry, Polish Academy of Sciences, Niezapominajek St. 8, 30-239 Cracow, Poland

Received December 14, 2006

Abstract: CASSCF/CASPT2 ab initio formalism has been applied to a thiolate model of cytochrome P450 compound I. A_{2u} ground state of porphyrin radical character was found in agreement with experimental results. A strong mixing of CASSCF reference states in multistate CASPT2 was observed, which is an interesting phenomenon, rare for the ground state near the equilibrium geometry. Details of the CASSCF/CASPT2 procedure (including the construction of the active space) are discussed. Parallel DFT calculations revealed that relative energies and the scheme of spin coupling are qualitatively reproduced by hybrid DFT (B3LYP); however, results from nonhybrid functionals (BLYP, BP86) are significantly different in these aspects.

1. Introduction

Cytochrome P450 (CYP) is a ubiquitous oxygenase of high biological importance. Its elusive active form, so-called compound I (Cpd I), is one of the strongest oxidants in biology.[1] Chloroperoxidase (CPO) is another enzyme forming Cpd I of similar structure in the active site; the common and specific feature of these two systems is the coordination of heme Fe via S of cysteine.

The electronic structure of low-lying states of the Cpd I, crucial for predicting and understanding its reactivity, was extensively studied, however, almost exclusively by means of density functional theory (DFT) and mostly using hybrid functionals (e.g., B3LYP).[2] In view of these results, low-lying electronic states of Cpd I arise from the coupling between *three unpaired electrons* located on the oxyferyl-porphyrin active site. Two of them occupy antibonding π^* orbitals of oxyferryl (FeO) moiety and couple to triplet configuration (*uu*). The third unpaired electron (of free-radical nature) couples with the triplet either ferro- or antiferromagnetically, consequently yielding quartet (*uuu*) or doublet (*uud*) configuration. This coupling is rather weak and may be described in terms of the Heisenberg Hamiltonian $H = -J\vec{S}_1\vec{S}_2$. In some calculations the third electron (radical) is located on the highest a_{2u} orbital of the porphyrin ring, whereas in others—on the $3p_\pi \equiv \pi_S$ lone pair of the axial *S* from cysteine, perpendicular to the Fe−S axis. In other words, two types of states of different radical and thus of different chemical characters exist. The states are conventionally labeled as $^{2,4}A_{2u}$ and $^{2,4}\Pi_S$. Relative energies of these porphyrin- and sulfur-radical states were shown[2,3] to be strongly dependent on the basis set and the functional used as well as on the environment of the active site considered in the computational model (vacuum, polarizable continuum, or explicit molecules in the nearest neighborhood).

Experimental studies on Cpd I of P450 are difficult due to the elusiveness of the active form; however, recently Kellner et al.[4] showed using UV−vis spectroscopy that the ground state is of a porphyrin radical nature. The same conclusion was drawn for CPO Cpd I by Rutter et al.[5] by means of EPR and Moesbauer and by Hosten et al.[6] using Resonance Raman spectroscopy.

† Dedicated to Professor Dennis R. Salahub on the occasion of his 60th birthday.

* Corresponding author e-mail: broclawi@chemia.uj.edu.pl.

10.1021/ct600363a CCC: $37.00
Published on Web 03/31/2007

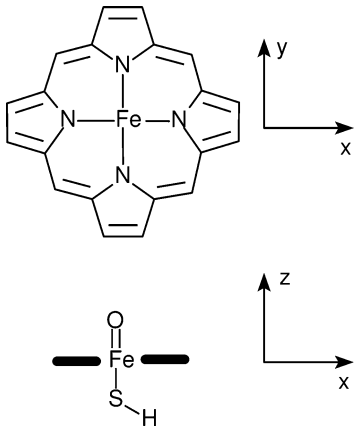

Figure 1. Top and side view of the Cpd I model system used in this study.

In this paper we focus on the description of Cpd I electronic structure by means of various methods: CASSCF/CASPT2,[7,8] hybrid DFT (B3LYP), and nonhybrid DFT (BLYP, BP86). The CASSCF/CASPT2 method—the main formalism presented—may be useful in resolving doubts arising from DFT methodology. It was chosen as a relatively low-cost and a rather reliable ab initio method,[9] which includes explicitly static and dynamic correlation, and is capable of describing a multiconfigurational nature of antiferromagnetic doublets properly.

2. Methods and Models

All calculations concern the idealized model system of the Cpd I active site [Fe(O)(SH)Por] having C_S symmetry (see Figure 1). This model has been already verified at the B3LYP level[10] as a good mimic of the Cpd I active site (providing similar relative energies as a full-cysteine model). Due to symmetry the states of interest belong to distinct representations of C_S:$^{2,4}\Pi_S \in A'$ while $^{2,4}A_{2u} \in A''$. According to the formal symmetry group (C_S) there are only two representations (A', A''); however, in this work all states are conventionally labeled after the location of free radical. Porphyrin-centered molecular orbitals are traditionally called a_{2u}, a_{1u}, e_g. Actually these orbitals are only slightly perturbed by the lowering of symmetry in our system. Thus A_{2u}, Π_S etc./a_{2u}, π_S etc. are not formal symmetry irreps but *conventional* labels of states/orbitals.

2.1. DFT Calculations. Unrestricted DFT geometry optimizations were performed with symmetry constrains for $^2\Pi_S$, $^4\Pi_S$ (lowest doublet and quartet of A' symmetry) and for $^2A_{2u}$, $^4A_{2u}$ (lowest doublet and quartet of A'' symmetry). For the B3LYP functional (using Gaussian03[11]) two basis sets were tested: one composed of ANO-S (6s4p3d2f)[12] for Fe and cc-pVDZ for other atoms (called below BS1) and the second—6-311G**—for all atoms (BS2). Similar calculations were repeated with BLYP and BP86 functionals (using the ADF suite[13]) in a comparable *n*ZP basis set of ADF: TZP for Fe and DZP for other atoms.

Vacuum geometries were used to estimate environmental effects in the frame of DFT by means of the simplest possible model—self-consistent reaction field (SCRF) of solvent with $\epsilon = 5.6$.[3] In this work SCRF calculations serve only to analyze general trends induced by polarizable environment and are treated rather qualitatively. Due to availability, the PCM model[14] was used in Gaussian03 and COSMO[15] in ADF.

2.2. CASSCF/CASPT2 Calculations. CASSCF/CASPT2 calculations were performed at equilibrium DFT geometries using the Molcas[16] suite in the ANO-S basis set[12] (contracted to 6s4p3d2f for Fe, to 4s3p2d for S, to 3s2p1d for N, C, O, and to 2s1p for H). The imaginary level shift 0.1 au was applied (to justify this choice the influence of level shift was analyzed).

Our primary goal in selecting active orbitals was to describe all of the lowest states appearing in DFT (i.e., $^{2,4}A_{2u}$, $^{2,4}\prod_S$). Additionally, two other porphyrin-radical states were of interest: $^{2,4}A_{1u}$. This was motivated by the results of Hosten et al.[6] suggesting that CPO Cpd I might have an unpaired electron in a_{1u} instead of the a_{2u} orbital of porphyrin.

The following orbitals were active in CASSCF (we postpone the detailed discussion of this choice to section 3.2.3): (1) π^*_{xz}, π^*_{yz}, π_{xz}, π_{yz}, $\sigma^*_{z^2}$, σ_{z^2} (located mainly on FeO moiety), (2) π_S, σ_S (located mainly of S), and (3) a_{2u}, a_{1u}, and pair of e_g (four frontiers of porphyrin ring). Contours of these orbitals are presented in Figure 2.

While computing the quartets of A'' irrep ($^4A_{2u}$, $^4\sum_S$) one orbital (π_S) was excluded because it was not participating in any state included in the state-average CASSCF and therefore had the tendency to rotate out of the active set (and become inactive).

Our calculation flow consists of State-Average CASSCF (SA-CASSCF) followed by Multi-State CASPT2 (MS-CASPT2).[17] MS-CASPT2 is a generalization of a "normal", so-called State-Specific CASPT2 (SS-CASPT2) approach. In the MS-CASPT2 method the correlation effects are estimated (up to the second order) for several SA-CASSCF states collectively. The states are coupled via an effective Hamiltonian and allowed to mix. The possibility of mixing can make up for some limitations of the active space, manifesting in inaccurate SS-CASPT2 energies due to deficiencies in CASSCF states.[17] Resulting linear combinations of CASSCF eigenvectors are called *Perturbatively-Modified (PM) states*. We should stress that they are not the final CASPT2 wave functions but only proper combinations of reference states from CASSCF which yield final wave functions after applying the CASPT2 wave operator.

The SA-CASSCF procedure was applied for each irrep and multiplicity to cover the states of interest: $^{2,4}\Pi_S$, $^{2,4}A_{1u}$, $^{2,4}A_{2u}$. As will be shown in section 3.2.1, some of them appear in CASSCF at relatively high energies (this is due to not including dynamic correlation yet). In other words, at the CASSCF level there are other states with energies between the lowest and the highest states of interest. For the sake of objectivity, we decided to include all these "intermediate" states in a state-average energy expression: in this way none of the prospective candidates for the ground state is ruled out a priori. According to the expectations, in the final MS-CASPT2, the "intermediate" states turned out to be higher in energy than the states of interest, *except for the* $^{2,4}\sum_S$ states—i.e. states analogous to $^{2,4}\Pi_S$ but with a radical in the $3p_\sigma \equiv \sigma_S$ orbital of sulfur. Results for $^{2,4}\sum_S$ will be given below as these states play an important role in further analysis.

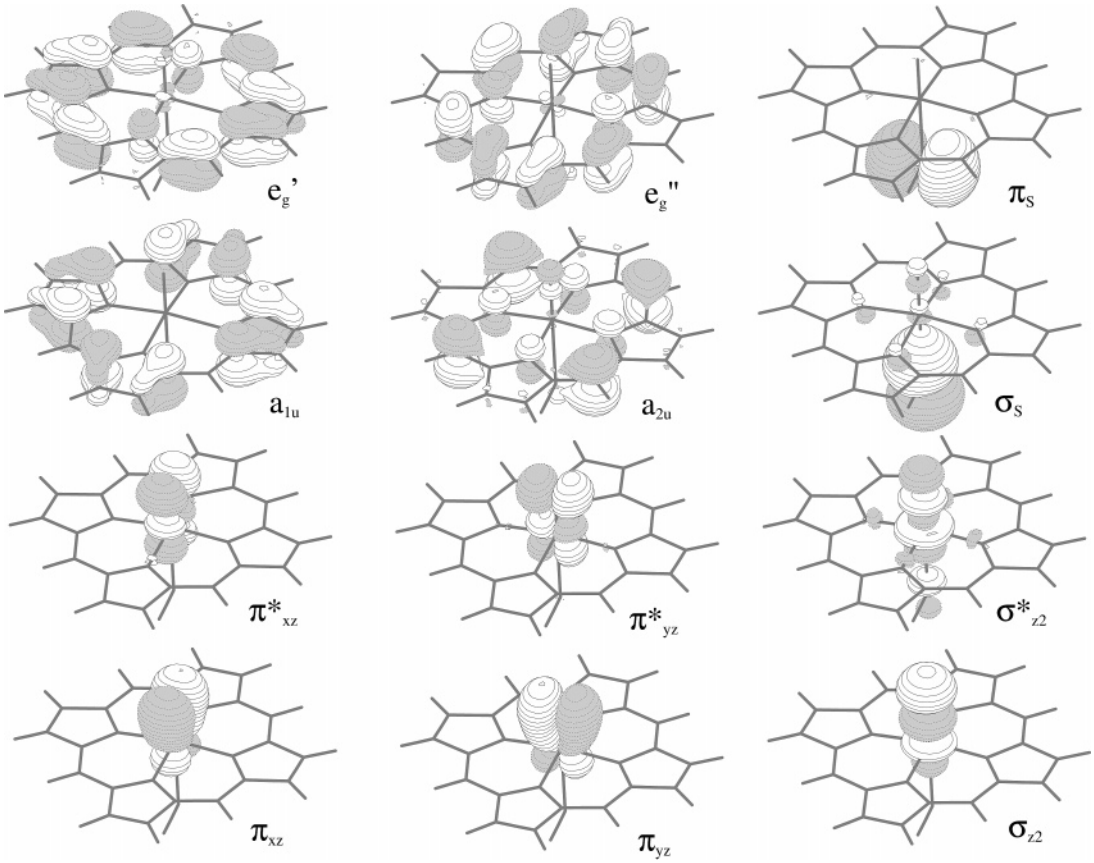

Figure 2. Contour plots of active orbitals.

2.3. Analysis of Properties. The coupling constant J was estimated for CASSCF/CASPT2 states simply as

$$J = \frac{2}{3}(E_d^{\mathrm{CAS}} - E_q^{\mathrm{CAS}}) \tag{1}$$

For Kohn−Sham wave-functions from unrestricted DFT the following formula (derived by Rodriguez and McCusker[18]) was employed due to spin contamination:

$$J = 2\frac{E_d^{\mathrm{DFT}} - E_q^{\mathrm{DFT}}}{\frac{3}{2}\left(\frac{3}{2}+1\right) - \langle \hat{S}^2 \rangle_d} \tag{2}$$

In the above formulas $\langle\ \rangle_d$ is the average value in the doublet state. E_d and E_q are the vertical energies of doublet and quartet (computed for the equilibrium geometry of the lower of them).

Spin distributions for unrestricted Kohn−Sham (UKS) orbitals were further analyzed by means of *natural spin orbitals*, which provide the leading one-electron contributions to spin density: in this analysis the molecular spin density is decomposed into squares of orbitals carrying excessive ↑ and ↓ spin. These orbitals are simply eigenvectors of spin density matrix, $P_\uparrow$ - $P_\downarrow$ (diagonalization should be done in orthonormal basis). Corresponding eigenvalues are called *occupation numbers* and may be associated with populations of excessive spin. An occupation number equals to +1 for one ↑ electron, to −1 for one ↓ electron, and to some real number between −1 and +1 in a general case. For unrestricted single determinantal methods the resulting occupations may be nontrivial since coefficients of UKS orbitals for ↑ and ↓ spins differ (this is also the reason why it is difficult to analyze excessive spin distribution only by inspecting UKS orbitals). *Natural orbitals*, defined (analogously) as eigenvectors of $P_\uparrow + P_\downarrow$, are complementary tools used to analyze the distribution of unpaired electrons. Contributions from "closed shells" are ≈ 2, from "virtual orbitals" ≈ 0 and ≈ 1 from orbitals carrying unpaired electrons.

Natural- and natural spin orbitals were computed from unrestricted orbitals using the original authors' program. Contour plots of orbitals and densities were prepared using Molden[19] and the Grid Viewer from the Molcas[16] suite. Small functionality was added to the Molcas code to enable extracting natural spin orbitals for PM states (used to compute spin densities for PM states).

3. Results and Discussion

3.1. DFT Modeling. B3LYP equilibrium geometries are included in the Supporting Information (see section 6). Adiabatic energies and exchange coupling constants for three examined functionals are given in Table 1.

According to our B3LYP results—being in general agreement with literature studies employing this functional[2,10]—the ground state is porphyrin radical (A_{2u}), both in vacuum and polar environment. The type of coupling strongly depends on the environment and on the basis set used, which makes a conclusive assignment of multiplicity difficult.[2,3] Nevertheless, for the hybrid functional the coupling is *weak* in all cases, about 0.1 kcal/mol, i.e., an order of

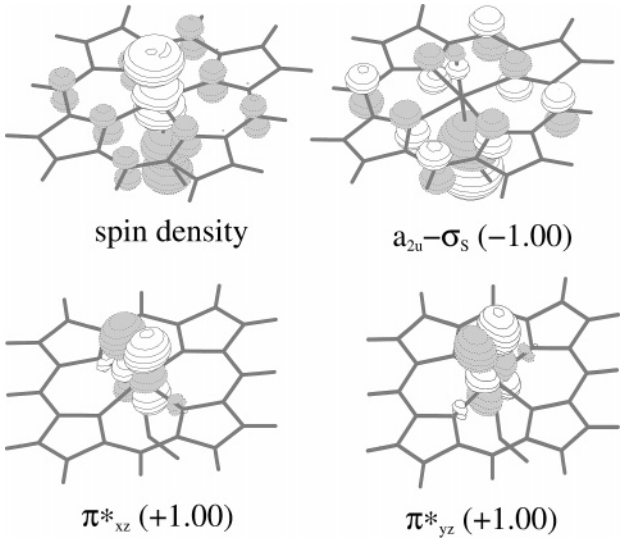

Figure 3. Contour plots of spin density and natural spin orbitals corresponding to three unpaired electrons for the $^2A_{2u}$ state, obtained from B3LYP/BS1 KS orbitals.

Table 1. Relative Adiabatic Energies (E_{ad}) and Coupling Constants (J), All in kcal/mol, for Various Functionals in Vacuum and SCRF

	B3LYP/BS1		B3LYP/BS2		BLYP		BP86	
	vac	SCRF	vac	SCRF	vac	SCRF	vac	SCRF
$E_{ad}(^2A_{2u})$	0.1	0.0	0.0	0.1	1.8	0.1	2.5	0.0
$E_{ad}(^4A_{2u})$	0.0	0.1	0.0	0.0	3.1	0.0	5.0	0.7
$E_{ad}(^2\Pi_S)$	3.1	5.3	3.4	6.0	0.0	2.2	0.0	1.3
$E_{ad}(^4\Pi_S)$	3.3	5.5	3.4	5.8	4.6	5.5	5.5	5.3
$J(A_{2u})$	0.06	−0.16	−0.03	0.05	−2.23	0.04	−3.32	−2.89
$J(\Pi_S)$	−0.12	−0.11	0.06	0.07	−2.49	−1.89	−2.94	−2.43

magnitude smaller than the separation between different types of radicals. In contrast to B3LYP, two nonhybrid functionals examined yield a different pattern of energies: not only the vacuum ground-state radical character is different but also J is much bigger (on the order of 2 kcal/mol, comparable to the separation of porphyrin and sulfur radicals). The influence of the polar environment yields generally the stabilization of $^{2,4}A_{2u}$ states for all potentials; however, this effect is much more clear for B3LYP than for BLYP and BP86.

According to spin distributions depicted in the first plots of Figures 3 and 4 (for doublets, in B3LYP) interacting spins are well separated in space—thus one would expect *weak exchange interaction*. However, in view of Table 1 this physically intuitive picture of weak spin-coupling occurring in two different types of radicals ($^2\Pi_S$ or $^2A_{2u}$) is supported only by the hybrid functional (B3LYP), while nonhybrid ones lead to a qualitatively different description.

Low-spin (doublet) states were carefully analyzed by means of natural spin orbitals. Three such orbitals, with eigenvalues closest to ±1, are depicted in Figures 3 and 4. All others have much smaller eigenvalues and are of minor importance for qualitative analysis.

The presented orbitals originate from B3LYP, but their spatial contours are quite similar for all functionals tested. However, eigenvalues (occupation numbers) *do differ significantly* (Table 2): for B3LYP there are three values close to "ideal" +1, +1, −1 describing the antiferromagnetic coupling of $S_1 = 1$ with $S_2 = 1/2$, which supports nicely the three electron model. [In principle, electronic configuration describing this coupling is three-determinantal: $|uud\rangle = (1/\sqrt{6})\ (2|\uparrow\uparrow\downarrow\rangle - |\uparrow\downarrow\uparrow\rangle - |\downarrow\uparrow\uparrow\rangle)$ and yields natural spin orbitals with eigenvalues +2/3, +2/3, −1/3, similar to those indeed found in CASSCF/CASPT2. However, in one-determinantal approximation this type of coupling is best described by $|\uparrow\uparrow\downarrow\rangle$ configuration, having spin orbitals with +1,+1,−1 eigenvalues.] For spin orbitals from BLYP and BP86 only one eigenvalue is close to +1, while all others have much smaller absolute values. A similar observation holds for natural orbitals (Table 3): again, in B3LYP their occupations are close to 1, 1, 1 (three unpaired electrons), while BLYP and BP86 give numbers rather closer to the following: 2 (electronic pair), 1 (single unpaired electron),

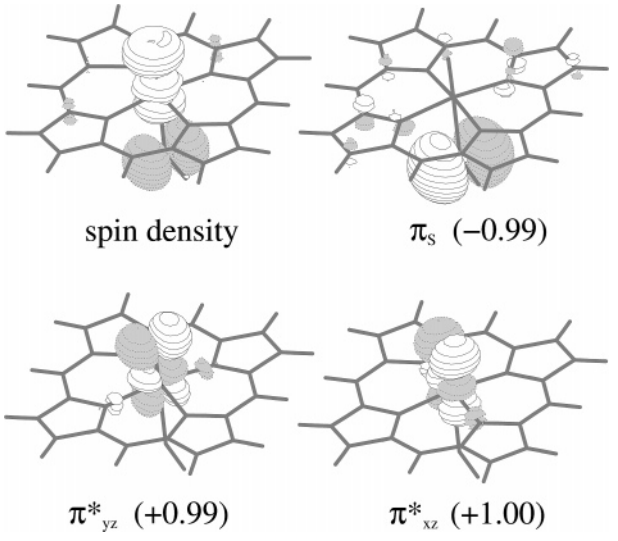

Figure 4. Contour plots of spin density and natural spin orbitals corresponding to three unpaired electrons for the $^2\Pi_S$ state, obtained from B3LYP/BS1 KS orbitals.

Table 2. Selected Natural Spin Orbitals (with Occupation Numbers Closest to ±1) for Doublet States from Various DFT Models

	$^2A_{2u}$			$^2\Pi_S$		
functional	π^*_{xz}	π^*_{yz}	$a_{2u}-\sigma_S$	π^*_{yz}	π^*_{xz}	π_S
B3LYP/BS1	1.00	1.00	−1.00	0.99	1.00	−0.99
B3LYP/BS2	1.00	1.00	−1.00	1.00	1.00	−1.00
BLYP	0.68	1.00	−0.68	0.68	1.00	−0.68
BP86	0.52	1.00	−0.52	0.66	1.00	−0.66

Table 3. Selected Natural Orbitals (with Occupation Numbers Closest to 1) for Doublet States from Various DFT Models

	$^2A_{2u}$			$^2\Pi_S$		
functional	$a_{2u}-\sigma_S$	π^*_{yz}	$\pi^*_{xz}+\sigma_S$	$\pi^*_{yz}-\pi_S$	π^*_{xz}	$\pi_S+\pi^*_{yz}$
B3LYP/BS1	0.98	1.00	1.02	0.89	1.00	1.11
B3LYP/BS2	0.97	1.00	1.03	0.97	1.00	1.03
BLYP	0.26	1.00	1.74	0.27	1.00	1.73
BP86	0.14	1.00	1.86	0.25	1.00	1.75

Table 4. SS- and MS-CASPT2 Vertical Energies (at B3LYP/BS1 $^2A_{2u}$ Geometry) for the States of Interest

relative energy [kcal/mol]			
SS-CASPT2		MS-CASPT2	
$^2\Pi_S$	0.0	$1^4(A_{2u}, \Sigma_S)$	0.0
$^4\Sigma_S$	1.0	$1^2(A_{2u}, \Sigma_S)$	0.9
$^4\Pi_S$	1.3	$^2\Pi_S$	8.2
$^2\Sigma_S$	5.4	$^4\Pi_S$	9.6
$^2A_{2u}$	8.1	$^2A_{1u}$	22.9
$^4A_{2u}$	11.4	$^4A_{1u}$	25.2
$^2A_{1u}$	14.6	$2^2(A_{2u}, \Sigma_S)$	27.4
$^4A_{1u}$	16.9	$2^4(A_{2u}, \Sigma_S)$	28.9

and 0 (vacant orbital). It follows that the "occupation schemes" exhibited by KS determinants from tested nonhybrid potentials are inconsistent with three unpaired electrons model of Cpd I. More precisely, occupation numbers obtained for nonhybrid DFT suggest the important contribution of another doublet configuration—with only one unpaired electron located on FeO. However, CASSCF/CASPT2 does not confirm any such doublet configuration (see below)—in fact the CASSCF/CASPT2 results are quite similar to the B3LYP ones. In the authors' opinion, the reported difference between functionals is an artifact of BLYP and BP86 arising from a bad description of exchange in these nonhybrid potentials.

3.2. CASSCF/CASPT2 Modeling. 3.2.1. Vertical Energies. In the first step, vertical energies for all states were computed at the $^2A_{2u}$ B3LYP/BS1 geometry (below we refer to these energies as "vertical"). Because the CASSCF method does not cover dynamic correlation one should not expect that experimental data can be understood by means of CASSCF energies. Indeed, at this level both porphyrin radical states are lying extremely high: $^{2,4}A_{2u}$ about 60−70 kcal/mol and $^{2,4}A_{1u}$ about 50 kcal/mol above the lowest state, which is $^2\Pi_S$ (with a quartet of only 3 kcal/mol above). On the other hand, $^{2,4}\Sigma_S$ states are relatively low-lying (about 10 kcal/mol above and the lowest state) and are the lowest doublet and quartet states in A'' irrep, instead of $^{2,4}A_{2u}$ being the lowest states of this irrep in DFT! SS-CASPT2 corrects this poor result somewhat, because porphyrin-radical states become lowered more than the sulfur-radical ones, but the latter states are still lying lower (compare Table 4).

The interaction between reference states in MS-CASPT2 affects mostly $^{2,4}A_{2u}$ and $^{2,4}\Sigma_S$ which mix and form PM states (linear combinations) with comparable weights of two interacting components. These PM states are labeled symbolically as $1^{2,4}(A_{2u}, \Sigma_S)$ and $2^{2,4}(A_{2u}, \Sigma_S)$. Other states of interest are almost unaffected by the multistate procedure (preserve their character from CASSCF). Final energies are given in Table 4.

To analyze the *nature of resulting PM states*, their spin densities were compared with spin densities of the pure CASSCF reference states. Spin densities for doublets (more interesting for visual analysis) are presented in Figure 5.

They illustrate well in which way σ_S-type and a_{2u}-type radicals (observed in CASSCF) form states of mixed nature. This interstate mixing is understandable in view of the DFT

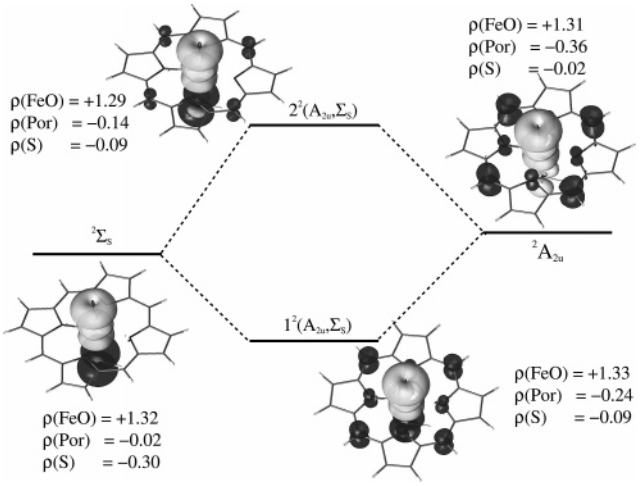

Figure 5. Contour plots of spin densities for CASSCF roots ($^2\Sigma_S$, $^2A_{2u}$) and PM states ($1^2(A_{2u}, \Sigma_S)$, $2^2(A_{2u}, \Sigma_S)$). Mulliken spin populations of FeO, S, and a porphyrin ring are also given.

results—in fact, states from DFT previously labeled $^{2,4}A_{2u}$ contain the important Σ_S contribution (see Figure 3); therefore—to be in agreement with the CASSCF/CASPT2 notation—they should be labeled as $^{2,4}(A_{2u}, \Sigma_S)$.

At the MS-CASPT2 level the results become *consistent with experiment*: the ground state is a combination of A_{2u} and Σ_S having a partial but significant *porphyrin-radical nature* (compare Figure 5). One should be aware, however, that the extent of MS-CASPT2 mixing may generally depend on the selection of active orbitals and cannot be treated as a routine remedy to cover eventual errors due to poor active space. Some warnings and recommendations regarding this point are raised by Serrano-Andrés et. al.[20]

3.2.2. Multiplicity of the Ground State and the Coupling Constant *J*. From vertical energies computed so far, the doublet or quartet (A_{2u}, Σ_S) emerges as a ground state. The difference in energy between them is quite small, and the order of states is likely to change during the geometry optimization. Hence, to assign the multiplicity of the ground state one should, in principle, compare adiabatic energies obtained from geometry optimizations in the frame of MS-CASPT2. However, since analytical gradients are not available in CASPT2, this way is not practical. CASSCF equilibrium geometries are often used as approximations to CASPT2 ones—unfortunately this is also impossible in our case because the final wave function of MS-CASPT2 originates not from a single CASSCF root (as in an ordinary, single-state CASPT2) but from their linear combination (PM state). To the best of the authors' knowledge, no software capable of computing CASSCF gradients for such a combination exists. The third way—and the only possible one here—is to use equilibrium geometries from DFT (B3LYP). As was noted, the correspondence of B3LYP solutions to MS-CASPT2 PM states is rather good, thus the trick might work. Following this idea, the authors recomputed the energies of all states in the proper geometries (for example, $^4A''$ states, to which $^4A_{2u}$ belongs, were computed for the $^4A_{2u}$ B3LYP geometry). Unfortunately, it turned out that for some states "adiabatic energies" computed in such a way

were *higher* than vertical energies for the initial geometry! It means that in our case geometries from B3LYP cannot be treated as good approximations to "true" (i.e., optimal for MS-CASPT2) ones. For this reason, the above estimations of adiabatic energies are not discussed further.

Nevertheless, the question of whether the ground state is $1^2(A_{2u},\Sigma_S)$ or $1^4(A_{2u}, \Sigma_S)$ remains vital. To approach the answer, we compared the relative energies of the doublet and quartet at equilibrium geometries of the corresponding states from B3LYP. Results for the first geometry were already presented above (with the quartet ground state and $J = +0.61$ kcal/mol). For the second geometry, the ground state turned out to be a doublet with $J = -0.30$ kcal/mol. The absolute energy of this state is the lowest one among all the state energies computed in this work. Thus, according to the highest manageable level we have applied, the ground state is $1^2(A_{2u},\Sigma_S)$ and coupling is antiferromagnetic. However, this is not a firm conclusion, since for giving a definite answer true equilibrium geometries should be known. Unfortunately, as was noted, those from B3LYP do not even provide reasonable MS-CASPT2 adiabatic energies.

3.2.3. Discussion of the Active Space Selection, Multistate Methodology, and Level Shift Influence. The selection of active orbitals is a result of our extensive, preliminary research (not reported here). We started from the orbitals which are absolutely necessary for constructing states of interest: π^*_{xz}, π^*_{yz}, π_S, a_{2u}, a_{1u}. Porphyrin's LUMO (e_g) was added to improve the description of the porphyrin ring.

Due to strong static correlation in moiety, the bonding pair π_{xz}, π_{yz} has to be active as a counterpart of antibonding π^*_{xz}, π^*_{yz}. Similarly, strong correlation is associated with the σ component of the bond, i.e., orbitals σ_{z^2} and $\sigma^*_{z^2}$. If they are not active, then their contributions to second-order energy are much bigger than for any other orbital. In contrast, omitted *d* orbitals ($3d_{x^2-y^2}$, $3d_{xy}$) have rather small contributions to second-order energy—they are comparable or smaller than contributions of many omitted porphyrin π orbitals, which cannot be active due to size limitations. Furthermore, these two *d* orbitals do not change occupations in any of the states considered here: $3d_{xy}$ is (approximately) "doubly occupied", whereas $3d_{x^2-y^2}$ participates in "doubly occupied" and "vacant" molecular orbitals. [Here the terms "vacant" and "doubly occupied" are used to describe the occupation numbers *only in the leading* configuration.] Therefore, one can guess that eventual corrections due to making them active would approximately cancel in relative energies.

The sulfur σ_S orbital was added due to different reasons. Indeed, we have discovered that in CASSCF calculation for $^{2,4}A''$ with *active* a_{2u} and *inactive* σ_S these orbitals exchange ($a_{2u} \rightleftharpoons \sigma_S$), and, as a result, the state which originally was $^{2,4}A_{2u}$ becomes $^{2,4}\Sigma_S$! The only way we have found to avoid this rotation was to make both orbitals active.

The procedure applied in this study (i.e., SA-CASSCF followed by MS-CASPT2) has some drawbacks. First of all, the orbitals being optimized in the CASSCF level are common for all electronic states involved, and hence they are far from optimal for any of them. Therefore SA-CASSCF performs worse with respect to electronic correlation than single-state CASSCF. Second, as was already noted, within the applied approach geometry optimization is impossible, either at the SA-CASSCF or the MS-CASPT2 level. From similar reasons accounting for environmental effects is very problematic in SA-CASSCF (because of the optimization of dielectric cavity based on a selected CASSCF state). In spite of these problems and limitations, the multistate approach seems to be the method of choice in our case, since the character of the CASSCF solution is qualitatively incorrect, and the important component (A_{2u}) of the true ground state has very high CASSCF energy. If this high-lying CASSCF state is ignored, then one obtains $^{2,4}\Pi_S$ and $^{2,4}\Sigma_S$ as the lowest states in CASPT2, which the result is obviously wrong.

Table 5. MS-CASPT2 Energies of $1^{2,4}(A_{2u}, \Sigma_S)$ and $^{2,4}\Pi_S$ States for Two Choices of the Active Space: 15 in 12 and 11 in 8

	relative energy [kcal/mol]	
	15 in 12	11 in 8
$1^2(A_{2u}, \Sigma_S)$	0.9	0.0
$1^4(A_{2u}, \Sigma_S)$	0.0	1.1
$^2\Pi_S$	8.2	8.6
$^4\Pi_S$	9.6	7.8

To estimate and eventually reduce the problem of the worse description of electronic correlation due to the presence of many states in SA-CASSCF optimization, we attempted to reduce the number of CASSCF roots involved in state-average calculations. With this aim we excluded from the previous active space some orbitals which were nearly doubly occupied in the states of interest and hence seemed to be not crucial, i.e., e_g of porphyrin (for all interesting states) and consequently also a_{2u}, σ_S (for Π_S, $A_{1u} \in A'$) or a_{1u}, π_S (for Σ_S, $A_{2u} \in A''$). This reduction results in an "11 in 8" active space (the previous, bigger one is called "15 in 12"). Our experience from an "15 in 12" active space was that the presence of the removed orbitals merely generated many "intermediate" states in CASSCF (i.e., the states lying between the states of interest as mentioned in section 2.2), which states are of no importance for final conclusions. The MS-CASPT2 ground-state candidates $1^{2,4}(A_{2u}, \Sigma_S)$ and $^{2,4}\Pi_S$ for both active spaces are compared in Table 5. One can see that the ground-state character and separation between two types of radicals are almost unaffected. Although the multiplicity of the ground state is different than previously, we are not entitled to discuss such a small difference in energies without the geometry optimization. Once again the type of exchange coupling appears to be sensitive to computational parameters. Nevertheless, Table 5 fully supports our previous conclusions regarding the radical character of the ground state. Moreover, the mixing between the CASSCF states still occurs in MS-CASPT2 to a similar extent as previously.

Another question is the dependence of our results on level shift. This was answered by analyzing level shift influence (in range 0.05−0.25 au) on relative MS-CASPT2 energies, relative SS-CASPT2 energies, reference weights, and weights of CASSCF roots in PM states. [*Reference weight* is the weight of the CASSCF reference function in SS-CASPT2 solution.] Details of this analysis can be found in the Supporting Information (see section 6). It shows that our results are not suffering from an intruder state problem even

for the smallest level shift, and our previous choice of 0.1 au is strongly supported. Although some dependencies on level shift are observed, they are quite understandable (they may be qualitatively explained by considering the influence of level shifting on the fraction of dynamic correlation recovered in CASPT2).

4. Conclusions

In spite of the technical difficulties due to the problem size and the need to compute high-lying A_{2u} states a reasonable active space was found. We note that no successful studies on Cpd I at the CASSCF/CASPT2 level have been reported so far. The computed ground state has an expected porphyrin radical nature in agreement with experimental results. In contrast to predicting radical character, we do not pretend to determine multiplicity of the ground state (and coupling constant J) on the basis of the above results; answering this question would require knowledge of optimal geometries for PM states since we need to compare energies differing by 1 kcal/mol or less.

We note that to obtain proper radical character and energies of the states in CASPT2, high-lying A_{2u} should be included in SA-CASSCF, and multistate treatment in CASPT2 is mandatory. Then, ab initio treatment of P450 or CPO Cpd I is possible, but there are important problems (not rooted solely in the size of the system), which had to be solved. Experience gained from this study might be useful in eventual future research employing bigger active spaces (e.g., having all d orbitals of Fe active).

It follows that the B3LYP ground state is analogous to the one found in CASSCF/MS-CASPT2 (e.g., by its spin density distribution, the electron coupling scheme, and the extent of mixing between sulfur and porphyrin radical). This agreement and observed big role of dynamic correlation—which dramatically changes identities and ordering of CASSCF states—provide a good forecast to use the B3LYP functional for similar systems. This simple method both describes exchange coupling rather well and has a dynamic correlation incorporated already in SCF (in contrast to the CASSCF/CASPT2 approach). However, one should be aware that nonhybrid functionals, with a worse description of exchange, applied to Cpd I may yield results that are qualitatively inconsistent with B3LYP and CASSCF/CASPT2 ones.

Acknowledgment. The computations were performed at the Academic Computer Centre CYFRONET AGH (computational grants no. MNiSW/SGI2800/UJ/133/2006 and MNiSW/SGI3700/UJ/133/2006). This work was partially sponsored by The Polish State Committee for Scientific Research (grant no. 2P04A 042 26). We thank Prof. K. Pierloot and Prof. B. O. Roos for valuable discussions and comments.

Supporting Information Available: B3LYP/BS1 equilibrium geometries and details of analysis of level shift influence on CASSCF/CASPT2 results. This material is available free of charge via the Internet at http://pubs.acs.org.

References

(1) Denisov, I. G.; Makris, T. M.; Sligar, S. G.; Schlichting, I. *Chem. Rev.* **2005**, *105*, 2253−2277.

(2) Shaik, S.; Kumar, D.; de Visser, S. P.; Altun, A.; Thiel, W. *Chem. Rev.* **2005**, *105*, 2279−2328.

(3) Ogliaro, F.; Cohen, S.; de Viser, S. P.; Shaik, S. *J. Am. Chem. Soc.* **2000**, *122*, 12892−12893.

(4) Kellner, D. G.; Hung, S.-C.; Weiss, K. E.; Sligar, S. G. *J. Biol. Chem.* **2002**, *277*, 9641−9644.

(5) Rutter, R.; Hager, L. P.; Dhonau, H.; Hendrich, M.; Valentine, M.; Debrunner, P. *Biochemistry* **1984**, *23*, 6809−6816.

(6) Hosten, C. M.; Sullivan, A. M.; Palaniappan, V.; Fitzgerald, M. M.; Terner, J. *J. Biol. Chem.* **1994**, *269*, 13966−13978.

(7) Roos, B. O.; Taylor, P. R.; Siegbahn, P. E. M. *Chem. Phys.* **1980**, *48*, 157−173.

(8) Andersson, K.; Malmqvist, P.-A.; Roos, B. O. *J. Chem. Phys.* **1991**, *96*, 1218−1226.

(9) Pierloot, K. *Mol. Phys.* **2003**, *101*, 2083−2094.

(10) Ogliaro, F.; Cohen, S.; Filatov, M.; Harris, N.; Shaik, S. *Angew. Chem., Int. Ed.* **2000**, *39*, 3851−3855.

(11) Frisch, M. J.; Trucks, G. W.; Schlegel, H. B.; Scuseria, G. E.; Robb, M. A.; Cheeseman, J. R.; Montgomery, J. A., Jr.; Vreven, T.; Kudin, K. N.; Burant, J. C.; Millam, J. M.; Iyengar, S. S.; Tomasi, J.; Barone, V.; Mennucci, B.; Cossi, M.; Scalmani, G.; Rega, N.; Petersson, G. A.; Nakatsuji, H.; Hada, M.; Ehara, M.; Toyota, K.; Fukuda, R. Hasegawa, J.; Ishida, M.; Nakajima, T.; Honda, Y.; Kitao, O.; Nakai, H.; Klene, M.; Li, X.; Knox, J. E.; Hratchian, H. P.; Cross, J. B.; Bakken, V. Adamo, C.; Jaramillo, J.; Gomperts, R.; Stratmann, R. E.; Yazyev, O.; Austin, A. J.; Cammi, R.; Pomelli, C.; Ochterski, J. W.; Ayala, P. Y.; Morokuma, K.; Voth, G. A.; Salvador, P.; Dannenberg, J. J.; Zakrzewski, V. G.; Dapprich, S. Daniels, A. D.; Strain, M. C.; Farkas, O.; Malick, D. K.; Rabuck, A. D.; Raghavachari, K.; Foresman, J. B.; Ortiz, J. V.; Cui, Q.; Baboul, A. G.; Clifford, S.; Cioslowski, J.; Stefanov, B. B.; Liu, G.; Liashenko, A.; Piskorz, P.; Komaromi, I.; Martin, R. L.; Fox, D. J.; Keith, T.; Al-Laham, M. A.; Peng, C. Y.; Nanayakkara, A.; Challacombe, M.; Gill, P. M. W.; Johnson, B.; Chen, W.; Wong, M. W.; Gonzalez, C.; Pople, J. A. *Gaussian 03, revision C.02*; Gaussian, Inc.: Wallingford, CT, 2004.

(12) Pierloot, K.; Dumez, B.; Widmark, P.-O.; Roos, B. *Theor. Chim. Acta* **1995**, *90*, 87−114.

(13) Baerends, E. et al. *ADF2004.01*; SCM, Theoretical Chemistry, Vrije Universiteit: Amsterdam, The Netherlands. http://www.scm.com (accessed December 2006).

(14) Cossi, M.; Rega, N.; Scalmani, G.; Barone, V. *J. Chem. Phys.* **2001**, *114*, 5691−5701.

(15) Klamt, A. *J. Phys. Chem.* **1995**, *99*, 2224−2235.

(16) Andersson, K. et al. *MOLCAS Version 5.4*; Lund University: Sweden, 2002.

(17) Finley, J.; Malmqvist, P.-A.; Roos, B. O.; Serrano-Andres, L. *Chem. Phys. Lett.* **1998**, *288*, 299−306.

(18) Rodriguez, J. H.; McCusker, J. K. *J. Chem. Phys.* **2002**, *116*,.

(19) Schaftenaar, G.; Noordik, J. *J. Comput.-Aided Mol. Des.* **2000**, *14*, 123−134.

(20) Serrano-Andrés, L.; Merchán, M.; Lindh, R. *J. Chem. Phys.* **2005**, *122*, 104107−104116.

CT600363A